

Simple Estimation of Average Field Strengths in Resonant Environments for Assessing Human Exposure to Electromagnetic Fields

Alastair R. Ruddle

Advanced Engineering Department, MIRA Limited,
Nuneaton, UK, Email: alastair.ruddle@mira.co.uk

Abstract—Simple estimates for average field strengths over the interior of a car due to an internal source are compared with detailed results from 3D numerical models. The effect of simple lossless window glass is also included in the analytical calculations. The comparisons demonstrate that reasonable estimates can be obtained for the car test case at frequencies above 1 GHz. This approach could be used to help assess field exposure in other resonant environments that are less amenable for detailed numerical simulation.

Keywords—average field strength; complex cavity; human exposure; power balance; dielectric filled apertures.

I. INTRODUCTION

Numerical models of a car and several occupants (represented by human-shaped homogeneous dielectric bodies) have been used to investigate SAR (specific absorption rate) and electromagnetic field distributions for an internal 400 MHz source [1]. The results suggest that whole-body average SAR limits are likely to be reached when the radiated power is high enough to produce average field levels over the interior of the empty vehicle that exceed the field reference levels of [2] by a factor of 1.95. This value compares favourably with numerical investigations based on anatomically detailed upright human simulants under plane wave illumination, where the safety factor provided by the field reference levels is around 2.25 at 400 MHz [3]. Thus, average internal field levels for empty vehicles could perhaps provide a useful measure for assessing possible human exposure threats for vehicle occupants.

Although 3D numerical modelling of a car is possible with relatively modest computing resources at 400 MHz, computing requirements remain a limitation for larger structures and higher frequencies. Thus, approximate methods that can provide reliable estimates for the average field levels in complex cavities could be of considerable benefit in assessing human exposure to electromagnetic fields. This paper presents a comparison

between simple estimates for the average field strengths inside a vehicle with results obtained from detailed 3D models based on CAD geometry. Although this study focuses on a car, average field estimates of this type could have wider applications in the assessment of human exposure threats for other resonant environments that are less amenable to detailed numerical simulation.

II. 3D NUMERICAL MODELS

The reference data for this investigation was obtained from 3D numerical models. These models were derived from CAD geometry for the body-shell and doors of passenger cars, as well as the major metallic parts in the passenger compartment (including the front and rear seat frames and interior steering components). All of these parts were approximated as perfect conductors. The simulations were carried out using a commercial TLM field simulation tool [4]. Models of this nature have shown good correlation with measurements of the local electric field distribution in the vicinity of a complete vehicle with an on-board 400 MHz transmitter [5].

Simple glazing with representative parameters was also included in some of the models, exploiting a thin film approximation to represent the dielectric layers more efficiently. For the models with glazing, all windows were assumed to have a relative permittivity of 6.5.

Using these models, average RMS field levels over the empty vehicle interior were derived from computed electric and magnetic fields at around two million points over the region that could be occupied by the passengers. Results for frequencies in the range 1–2 GHz were obtained from a vehicle model that was excited using a simple dipole antenna located in the vicinity of the rear seat, for both horizontal and vertical polarization. The values obtained for a radiated power of 1 W CW are detailed in Tables I–II, which also include data obtained at 400 MHz for a model of another vehicle of similar size. The latter did not include glazing and was excited with a slightly different source antenna, although in a similar location, but for horizontal polarization only.

This work was carried out as part of the SEFERE project, which is supported in part by the UK Government's Technology Strategy Board (Technology Programme reference TP/3/DSM/6/1/15266).

The results detailed in Table I show that the average field values from the 3D numerical models are at similar levels for frequencies above 1 GHz, and do not differ markedly between the two source polarizations. However, the values obtained at 400 MHz are lower than those obtained at the higher frequencies (by a factor of the order of $2^{1/2}$).

TABLE I. AVERAGE INTERNAL ELECTRIC FIELDS AT 1 W CW OBTAINED FROM 3D VEHICLE MODELS

Frequency (MHz)	Source polarization	Electric field (V/m, RMS)	Magnetic field (mA/m, RMS)
2000	Vertical	22.5	59.4
	Horizontal	22.9	60.7
1500	Vertical	23.3	61.6
	Horizontal	24.3	64.3
1000	Vertical	22.3	58.2
	Horizontal	22.7	59.5
400	Horizontal	17.4	45.0

III. ESTIMATES FOR VEHICLE WITHOUT GLAZING

Since the numerical model included only perfect conductors, the apertures provide the only source of loss for this system. Although there are many apertures in the vehicle body-shell, most of these features are relatively small. The windows are therefore the dominant apertures for the vehicle, and the primary source of loss.

The power $P_T(f)$ transmitted through an aperture of area A at frequency f under incident power density $S(f)$ per unit area is:

$$P_T(f) = T_A(f) S(f) A \quad (1)$$

where $T_A(f)$ is an aperture transmission coefficient that depends on the frequency, aperture geometry, angle of incidence and polarization. A method for estimating the transmission coefficient of a rectangular aperture under uniform illumination at normal incidence is given in [6], where it is reported that the transmission coefficients obtained for rectangular apertures are quite similar to those for square apertures. The transmission coefficient for a rectangular aperture with sides a and b [6] is:

$$T_A(f) = \frac{4abf^2}{c^2} \int_0^{\pi/2} \int_0^{\pi/2} [\alpha\beta]^2 \sin(\theta) d\theta d\phi \quad (2)$$

where c is the speed of light and:

$$\alpha = \frac{\sin\{\pi a f \sin(\theta) \cos(\phi) / c\}}{\pi a f \sin(\theta) \cos(\phi) / c} \quad (3)$$

$$\beta = \frac{\sin\{\pi b f \sin(\theta) \sin(\phi) / c\}}{\pi b f \sin(\theta) \sin(\phi) / c} \quad (4)$$

Vehicle windows are clearly not rectangular, but representative dimensions for the car windows were derived from CAD data for the vehicle and used to estimate transmission coefficients for rectangular apertures of similar dimensions. The values obtained for representative front, rear and side window dimensions (see Fig. 1) are within $\pm 6\%$ of unity for frequencies above about 300 MHz, and within $\pm 2\%$ from 1 GHz.

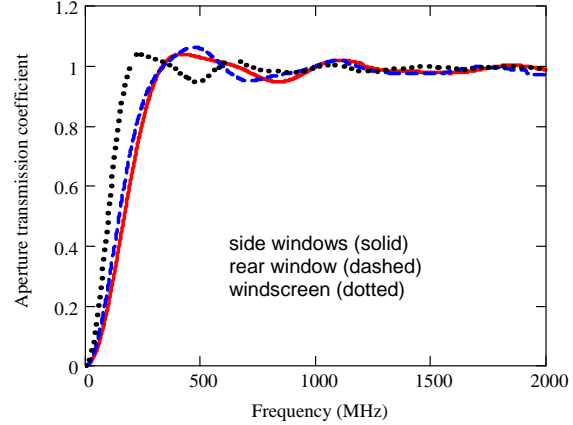


Figure 1. Normal incidence transmission coefficients for uniformly illuminated rectangular apertures with dimensions that are representative of car windows.

These results suggest that car windows can probably be regarded as electrically large at the frequencies of the numerical simulations (ie. 400 MHz to 2 GHz). For electrically large apertures, the transmission properties are independent of shape, frequency and polarization, and the average transmission cross-section (averaging over all angles of incidence) is equal to half the area of the aperture [7].

Assuming that the average electric and magnetic fields are related by the wave impedance of free space, the power $P_D(f)$ lost at frequency f through electrically large apertures of area A_k is then approximated by:

$$P_D(f) \approx \frac{1}{2} \frac{\langle E_{RMS}(f) \rangle^2}{120\pi} \sum_k \frac{A_k}{2} \quad (5)$$

where $\langle E_{RMS}(f) \rangle$ is the average RMS internal electric field strength and the factor $1/2$ reflects the assumption that only half of the power is represented by the angular spectrum of plane waves propagating towards any given aperture.

Using the power balance approach [7], the power radiated into the interior of the vehicle is equated with the power lost through the apertures. The average RMS internal electric field strength is then related purely to the radiated power $P_R(f)$ and the area of the windows via:

$$\langle E_{RMS}(f) \rangle \approx \sqrt{\frac{240\pi}{\sum_i (A_i/2)} P_R(f)} \quad (6)$$

The area of the car windows was also determined from the vehicle CAD data. The resulting estimates for the average fields were 21.7 V/m for the electric field and 57.6 mA/m for the magnetic field, normalized to a radiated power of 1 W CW. These values are remarkably close to those obtained from the detailed numerical models for frequencies of 1–2 GHz (see Table I).

The simple approach is found to overestimate the average internal fields at 400 MHz. Since the window apertures are thought to be large enough at 400 MHz to be approximated as “electrically large”, it seems more likely that the volume of the passenger compartment may not be sufficiently large for statistical arguments to be valid this frequency. At 400 MHz the overall dimensions of the cabin interior are only of the order of 1.3 x 2 x 2.7 wavelengths. This increases to 3.3 x 5 x 6.7 wavelengths at 1 GHz, rising to around 6.7 x 10 x 13.3 wavelengths at 2 GHz.

The amplitude distributions for the field components are expected to be of Rayleigh form in electrically large cavities, for which the probability and cumulative distribution functions are related to the mean values. The net field is expected to approach a Chi distribution with six degrees of freedom [8], characterized by the variance of the field components, which is also expected to be related to the mean RMS field:

$$\nu_E(f)^2 = \langle E_{RMS}(f) \rangle^2 / 6 \quad (7)$$

The amplitude probability distribution $P(E_{RMS})$ for the net electric field is therefore of the form:

$$P(E_{RMS}) = 27 \frac{E_{RMS}^5}{\langle E_{RMS} \rangle^6} \exp \left\{ -3 \left[\frac{E_{RMS}}{\langle E_{RMS} \rangle} \right]^2 \right\} \quad (8)$$

while the cumulative distribution $C(E_{RMS})$ is given by:

$$C(E_{RMS}) = 1 - \exp \left\{ -3 \left[\frac{E_{RMS}}{\langle E_{RMS} \rangle} \right]^2 \right\} \sum_{m=0}^2 \frac{3^m}{m!} \left[\frac{E_{RMS}}{\langle E_{RMS} \rangle} \right]^{2m} \quad (9)$$

The corresponding magnetic field distributions are estimated in a similar manner, assuming that the average electric and magnetic fields are related by the wave impedance of free space.

Sample amplitude probability and cumulative distributions for the net fields obtained from the 3D simulations are shown in Figs. 2-5, which also show the corresponding Chi distributions based on the average RMS field magnitudes estimated using (6) and (7). The distributions obtained from the numerical models are fairly similar between frequencies and between source polarizations. The Chi distributions based on the average field estimates are higher around the peaks of the amplitude probability distribution and lower at higher field levels. However, the vehicle interior is not strictly electrically large, and the region sampled from the numerical model includes the source as well as the metal elements of the steering wheel and front seat frames.

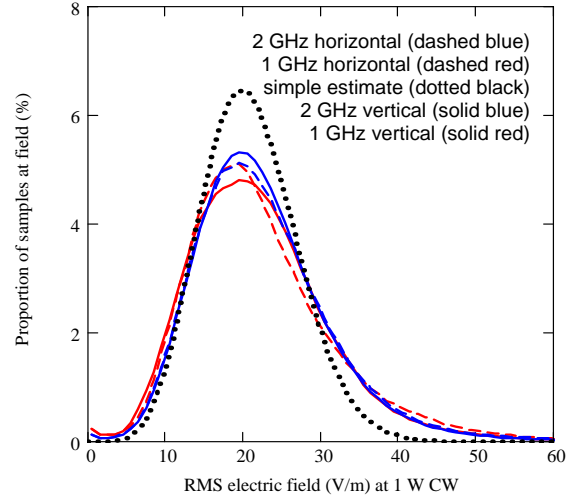


Figure 2. Amplitude probability distributions for electric field.

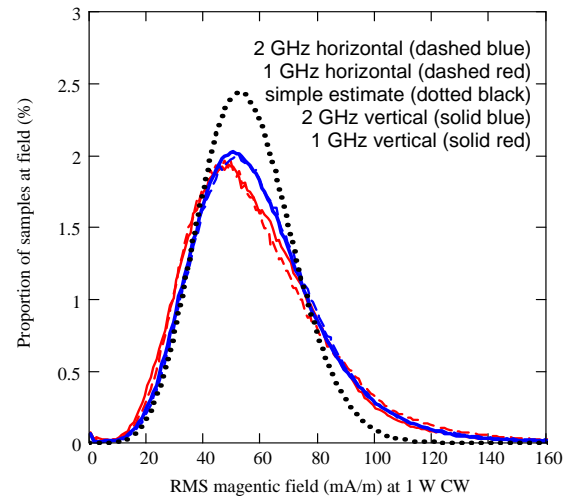


Figure 3. Amplitude probability distributions for magnetic field.

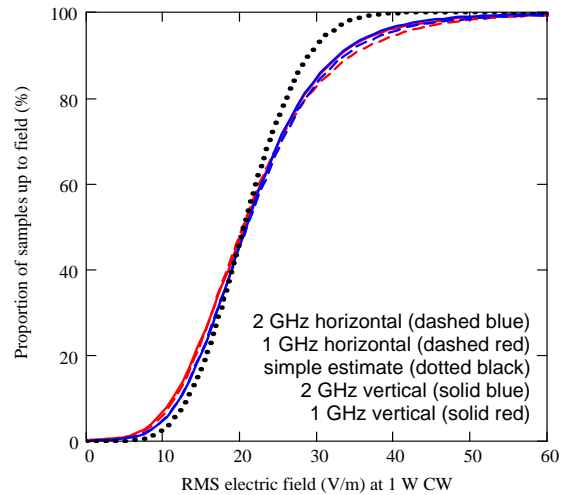


Figure 4. Cumulative distributions for electric field.

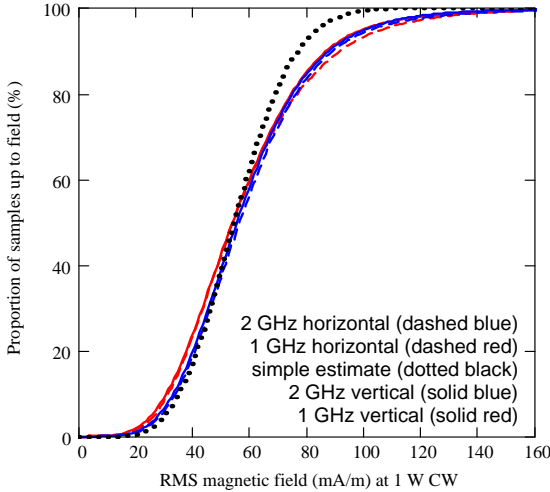


Figure 5. Cumulative distributions for magnetic field.

IV. INCLUDING GLAZING EFFECTS

Vehicle glazing is expected to have a greater impact at frequencies above 1 GHz, where the thickness may become resonant. Furthermore, the transmission properties of dielectric layers also depend on the field polarization and angle of incidence. Thus, a more detailed calculation is required in order to estimate the average internal field at microwave frequencies.

Simple window glass could be approximated as a planar slab of thickness d formed from a single non-magnetic material of relative permittivity $\epsilon(f)$ and zero conductivity. The effective transmittance for a particular field polarization p (ie. with the electric field either parallel or perpendicular to the plane of incidence) can then be obtained using:

$$T_p(f, d, \theta) = \left| \frac{t_{p1}(f, \theta)t_{p2}(f, \theta)\exp\{-i\delta(f, d, \theta)\}}{1 + r_{p1}(f, \theta)r_{p2}(f, \theta)\exp\{-i\delta(f, d, \theta)\}} \right|^2 \quad (10)$$

where the $r_{pi}(f, \theta)$ and $t_{pi}(f, \theta)$ represent the Fresnel reflection and transmission coefficients [9] corresponding to the particular polarization for the air-glass (denoted $p1$) and glass-air (denoted $p2$) interfaces, and θ is the angle of incidence in air.

The phase parameter $\delta(f, d, \theta)$ is given by:

$$\delta(f, d, \theta) = \frac{2\pi fd\sqrt{\epsilon(f)}}{c} \sqrt{1 - \frac{1}{\epsilon(f)}\sin^2(\theta)} \quad (11)$$

For frequencies where the glass is significant, (6) could be modified to account for the resulting loss in transmittance by introducing frequency dependent aperture weighting factors $w_k(f)$ such that:

$$\langle E_{RMS}(f) \rangle \approx \sqrt{\frac{240\pi}{\sum_k \left[\frac{A_k}{2} w_k(f) \right]}} P_R(f) \quad (12)$$

where the weighting factors $w_k(f)$ depend on the thickness and electrical properties of the window glazing.

Assuming that the energy is distributed equally between the two polarizations, the average transmission cross-section $\langle \sigma_k(f) \rangle$ (averaged over all possible angles of incidence) for an electrically large dielectric-filled aperture is estimated from:

$$\langle \sigma_k(f) \rangle = \frac{A_k}{2\pi} \int_0^{2\pi} d\phi \int_0^{\pi/2} \frac{[T_{k\perp} + T_{k\parallel}]}{2} \cos(\theta)\sin(\theta) d\theta \quad (13)$$

where $T_{k\perp}$ and $T_{k\parallel}$ are the transmittances for aperture k with the field perpendicular and parallel to the plane of incidence, respectively. Consequently, the weighting factors of (12) are given by:

$$w_k(f) = \int_0^{\pi/2} [T_{k\perp} + T_{k\parallel}] \cos(\theta)\sin(\theta) d\theta \quad (14)$$

Laminated glass could also be treated in a similar manner, by determining the effective transmittances for the multi-layer. The effects of finite losses could also be included by introducing a complex permittivity parameter where the real part reflects the relative permittivity and the imaginary component includes the conductivity. In this case it would also be necessary to estimate the power absorbed by the glass. This approach could also be applied to other types of dielectric boundary, such as brick and concrete walls of buildings.

The frequency dependence of the aperture weighting factor obtained from (14) is illustrated in Fig. 6, for glass of relative permittivity 6 at a range of thicknesses that are representative of vehicle glazing.

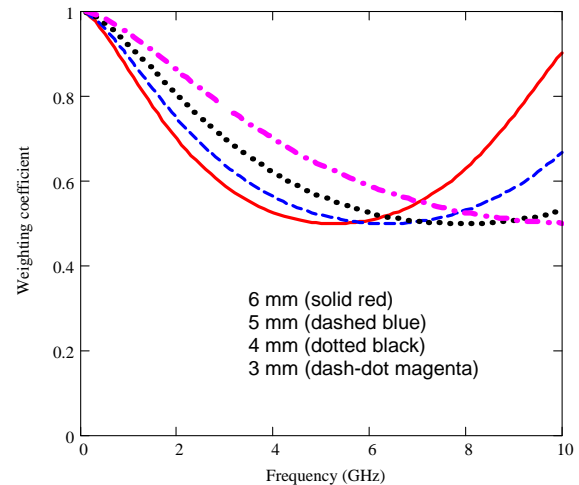


Figure 6. Aperture weighting factors for glass with a relative permittivity of 6 at various thicknesses.

The Q factor for the leaky cavity can be estimated from the volume and the total aperture transmission cross-section [7]. For a vehicle passenger compartment of volume V the Q factor is therefore estimated from:

$$Q(f) \approx \frac{8\pi V f}{c \sum_k [A_k w_k(f)]} \quad (15)$$

Determining the volume of the passenger compartment from CAD data is not easy, because of the complexity of the structure. However, a rough estimate gives the results shown in Fig. 7, which compare favourably with reported Q factors estimated from antenna transmission measurements carried out inside a complete car of a different type [10].

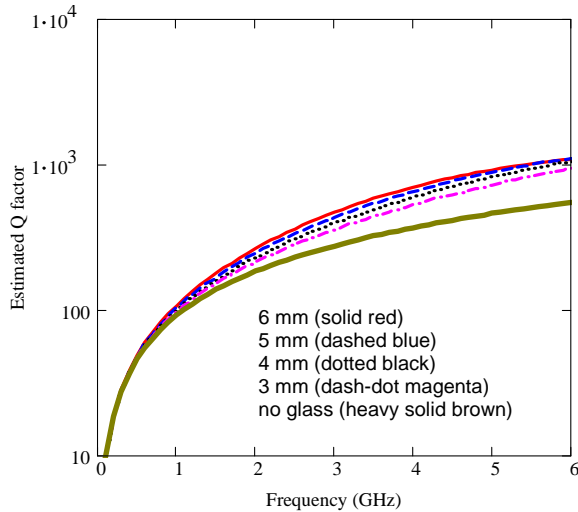


Figure 7. Estimated Q factor for vehicle model without glass (lower curve), and with glass of relative permittivity 6 at various thicknesses.

V. RESULTS FOR CAR MODELS WITH GLAZING

Using the approximate approach outlined above, the expected impact of lossless glass on the average internal electric field strength has been estimated for a number of glass thickness configurations (see Fig. 8).

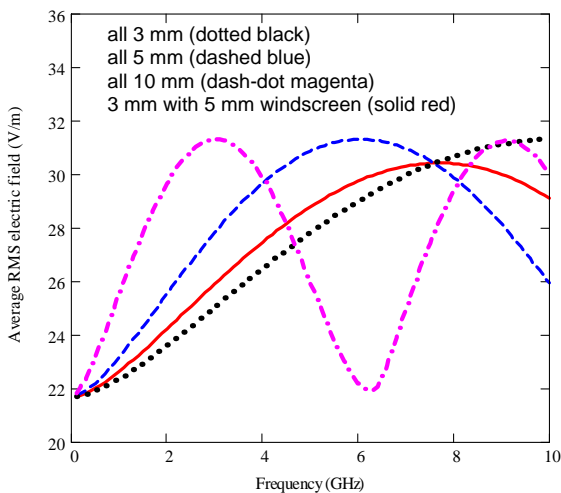


Figure 8. Estimated average internal electric field for 1 W CW source in perfectly a conducting vehicle with lossless glass.

For the most realistic scheme (5 mm windscreen with all other panels 3 mm thick), the estimated changes are only around 10% over the band 1–2 GHz. The results of the corresponding numerical simulations are of similar magnitude (see Table II). However, increases of up to 40% are predicted from the simple model, depending on the frequency and glass thickness. Consequently, Table II also includes estimates and results from numerical simulations for 1 cm thick glass. The latter are again of similar magnitude to the estimated averages despite the enormous difference in the computational effort and information requirements.

TABLE II. AVERAGE INTERNAL ELECTRIC FIELDS WITH GLASS

Glazing case	Frequency (MHz)	Net RMS electric field at 1 W CW (V/m)		
		Simple estimate	Numerical model of car with dipole source	
			Vertical	Horizontal
Windscreen 5 mm, all other glass 3 mm	1000	22.7	21.8	22.5
	1500	23.4	24.1	24.6
	2000	24.2	23.9	24.7
All glass 1 cm thick	1000	25.5	24.8	24.6
	1200	26.5	27.1	26.0
	1400	27.4	26.7	27.9
	1500	27.9	27.6	27.8
	1600	28.3	26.9	28.9
	2000	29.7	27.4	27.7

Sample amplitude distributions obtained from the numerical simulations and simple estimates for a vehicle with 1 cm thick lossless glass are shown in Fig. 9, in this case for the electric field at 2 GHz.

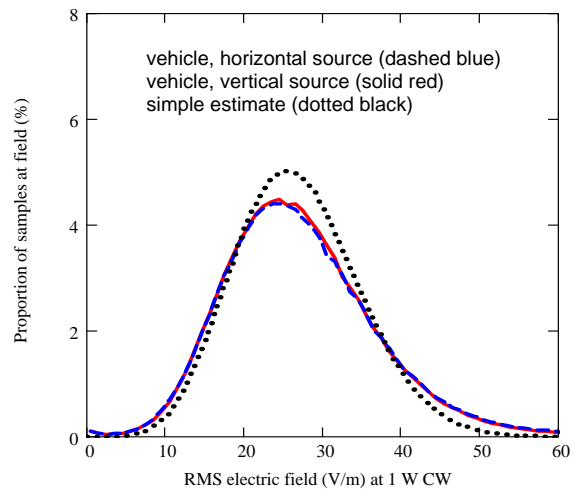


Figure 9. Amplitude distributions for 2 GHz electric field with 1 cm thick glass.

VI. IMPLICATIONS FOR IN-VEHICLE EXPOSURE

The electric field reference levels of [2] for general public exposure at frequencies in the range 400 MHz to 300 GHz are defined as follows:

$$E_{GP_REF}(f) = \begin{cases} 1.375\sqrt{f_{MHz}} & \text{for } 400 < f_{MHz} < 2000 \\ 61 & \text{for } 2 < f_{GHz} < 300 \end{cases} \quad (16)$$

where f_{MHz} and f_{GHz} represent the frequency in units of MHz and GHz, respectively, and $E_{REF}(f)$ is an RMS value intended to be averaged over a 6 minute period.

The CW power that would result in average internal electric fields reaching the reference levels can be projected from the 1 W average field estimates using:

$$P_{MAX_GP}(f) \approx \frac{E_{REF}(f)^2}{\langle E_{RMS}(f) \rangle^2}_{1W} \quad (17)$$

The results shown in Fig. 10 are based on the average electric field estimates for a car with and without glazing. The glass is assumed to be a single layer with a relative permittivity of 6.5 and no loss. The windscreen is 5 mm thick and all other windows are 3 mm thick. These projections include frequencies up to 10 GHz, which remain a challenging task for 3D numerical simulation.

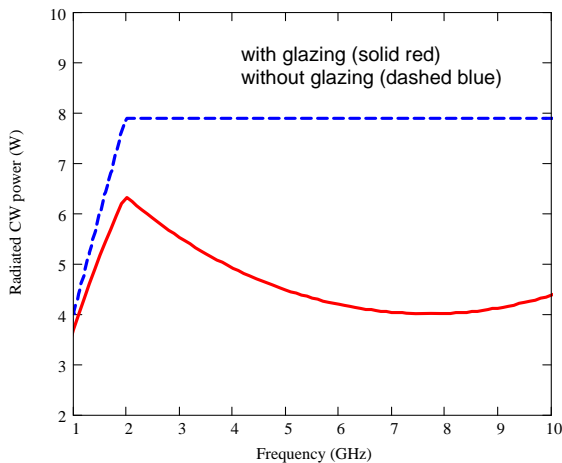


Figure 10. Estimated internal CW power expected to result in average fields inside a car that equal the reference levels of [2].

VII. CONCLUSIONS

A simple approach for estimating the average field strength inside a partial cavity with electrically large apertures, based purely on the area of the apertures and the power radiated inside, has been investigated as a possible alternative to numerical simulation. A method for extending these estimates to include the effects of dielectric materials in the apertures is also proposed.

The effectiveness of these methods has been evaluated against detailed 3D numerical models of the metal parts of a car, with and without glazing. The resulting estimates provide a remarkably good correlation

with values derived from the numerical simulations, given the enormous difference in the computational effort and information requirements. Simple estimates for the Q factor of a car also compare favourably with published results derived from antenna transmission measurements inside a complete vehicle.

The approximate approach is expected to become more reliable for larger structures and higher frequencies, which are also less amenable to deterministic numerical computation. This approach may therefore offer a very convenient way to assess likely compliance with field reference levels for a class of exposures arising from sources inside electrically large partial cavities. Possible applications could range from larger vehicles, including ships and aircraft, to other resonant environments such as buildings.

ACKNOWLEDGMENTS

The SEFERE project consortium includes MIRA Ltd (coordinator), ARUP Communications, BAE Systems Ltd, Harada Industries Europe Ltd, Jaguar Cars, UK National Policing Improvements Agency, University of Sheffield and Volvo Car Corporation (Sweden). Further information is available on the project website (see <http://www.sefere.org>).

REFERENCES

- [1] A.R. Ruddle, "Computed SAR distributions for the occupants of a car with a 400 MHz transmitter on the rear seat", Proc. 18th Zurich Int. EMC Symp., Munich, Germany, September 2007, pp. 37-40.
- [2] ICNIRP, "Guidelines for limiting exposure to time-varying electric, magnetic, and electromagnetic fields (up to 300 GHz)", Health Physics, Vol. 74, No. 4, 1998, pp. 494-522.
- [3] A.F. McKinlay et al, "Review of the scientific evidence for limiting exposure to electromagnetic fields (0-300 GHz)", Documents of the NRPB, Vol. 15, No. 3, 2004, pp. 142-145.
- [4] D.P. Johns, R. Scaramuzza and A.J. Wlodarczyk, "Micro-Stripes - microwave design tool based on 3D-TLM", Proc. 1st Int. Workshop on Transmission Line Matrix (TLM) Modeling - Theory and Applications, Victoria, Canada, August 1995, pp. 169-177.
- [5] A.R. Ruddle, "Validation of predicted 3D electromagnetic field distributions due to vehicle mounted antennas against measured 2D external electric field mapping", IET Proc. Sci., Meas. and Technol., Vol. 1, No. 1, January 2007, pp. 71-75.
- [6] G.F. Koch and K.S. Kolbig, "The transmission coefficient of elliptical and rectangular apertures for electromagnetic waves", IEEE Trans. Ant. Prop., Vol. 16, No. 1, January 1968, pp. 78-83.
- [7] D.A. Hill, M.T. Ma, A.R. Ondrejka, B.F. Riddle, M.L. Crawford and R.T. Johnk, "Aperture excitation of electrically large, lossy cavities", IEEE Trans. EMC, Vol. 36, No. 3, August 1994, pp. 169-178.
- [8] J.G. Kostas and B. Boverie, "Statistical model for a mode-stirred chamber", IEEE Trans. EMC, Vol. 33, No. 4, November 1991, pp. 366-370.
- [9] H.M. Liddel, "Computer-aided Techniques for the Design of Multilayer Filters", Adam Hilger, Bristol, 1981, pp. 7-8.
- [10] M. Heddebaut, C. Gransart, J. Rioult, and V. Deniau, "WxAN communication effectiveness inside vehicle bodies, in presence of passengers", Proc. EuroEMC Workshop on EMC of Wireless Systems, Rome, Italy, September 2005, pp. 118-121.